



# Simulation experiment on the Uplift and Tilt Correction of Buildings through Grouting Strengthening

Yunxuan Bi<sup>\*</sup>, Hanming Zhang<sup>a</sup>

College of Engineering and Technology, China University of Geoscience, Beijing, 100083, China

<sup>a</sup>1002201303@cugb.edu.cn, <sup>\*</sup>yunxuanbi@gmail.com

**Abstract.** Practical experience in underground construction has shown that the grouting uplift and tilt correction technique is more effective in addressing structural tilting issues that arise during construction. In order to enhance the study of the strengthening effects during the grouting uplift process, this research conducted indoor simulated grouting experiments to systematically analyze the consolidation grouting uplift mechanism. The study also examined changes in the physical and mechanical properties of the soil during the grouting process. Experimental validation confirmed that post-grouting, soil samples exhibited an increase in shear strength and density, also a decrease in water content and porosity. This affirms the effectiveness of consolidation grouting in achieving uplift and establishes certain patterns of soil sample reinforcement through grouting. The results of this study hold significance for engineering practice.

**Keywords:** Tilt correction; Grouting uplift; Compaction grouting; Simulation experiment

## 1 Introduction

In this era, urbanization is dramatically burgeoning, and the development and utilization of underground space in urban areas became a preponderant way to alleviate the scarcity of urban resources and improve environmental conditions [1]. According to the research by Ge Jianguo and others on the analysis of the reasons for the tilting of existing buildings, underground construction projects for instance urban subways and underground tunnels can potentially induce ground settlement, leading to building subsidence, cracking, and tilting [2], even posing serious safety hazards.

The improvement for tilt rectification of existing buildings is currently an all-important technique for improving their functional use [3]. In order to verify the influence of grouting uplift in actual projects, some scholars have done relevant field tests in actual grouting projects[4]. Based on various studies, including on-site research on the effectiveness of compaction grouting at Tokyo International Airport [5], conducted by EI Kelesh Adel M and others, compaction grouting has been affirmed as an effective method for soil and foundation improvement, reducing ground settle

© The Author(s) 2023

H. Bilgin et al. (eds.), *Proceedings of the 2023 5th International Conference on Civil Engineering, Environment Resources and Energy Materials (CCESEM 2023)*, Advances in Engineering Research 227,

[https://doi.org/10.2991/978-94-6463-316-0\\_41](https://doi.org/10.2991/978-94-6463-316-0_41)

ment, and raising the ground surface and existing structures. It can effectively avenge the limitations of traditional building correction techniques such as excavation, anchor-jacked piles uplifting, and other methods suitable only for lightweight buildings, which can precipitate fatal secondary damage to foundations and structures. However, as demonstrated by Wang Guangguo and others in their study on the mechanism and effectiveness of compaction grouting [6], there is still a dearth of indoor simulation testing for compaction grouting.

The approach of understanding the mechanisms and parameters that control compaction grouting has been to evaluate the results of fullscale injection tests and completed projects[7]. Therefore, this study analyzes the mechanism of compaction grouting and conducts indoor simulation grouting tests to explore the strengthening effect on the soil during the grouting and lifting process of buildings. It systematically investigates the changes in the mechanical and physical properties of the soil caused by grouting and lifting under certain grouting parameters, providing experimental guidance for on-site grouting and lifting reinforcement construction.

## 2 Theoretical analysis

### 2.1 Mechanism Analysis Overview

The grouting uplift and tilt correction process can be divided into two steps: the grout compaction phase and the lifting phase. In the grout compaction phase, under high grouting pressure, the grout compacts the surrounding foundation soil without invading the solid. This process creates elastic and plastic zones within a certain range, engendering the compression of soil pores, and waxing soil compression modulus. Particularly in cohesive soil foundations, the grouting pressure can generate excess pore water pressure. Once this excess pore pressure dissipates, the soil undergoes consolidation, leading to an increase in its compressive and shear strength.

The lifting phase is shown in Figure 1, when the grouting pressure reaches the lifting threshold, a conical failure zone appears above the grout pocket, causing the ground to rise, and subsequently lifting the building to correct its tilt. The grouting pressure primarily focuses on lifting the upper rudimentary soil and the building's foundation structure. The strengthening effect on the soil is somewhat reduced compared to the first step.

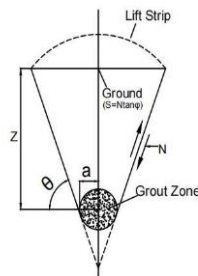


Fig. 1. Schematic Diagram of the Uplift Stages

### 3 Test design and process

#### 3.1 Experimental Principles and Design

This experiment is based on the mechanism of consolidation grouting uplift and is designed to study a single influencing factor using indoor model testing. Homogeneous soil samples are employed, and the expansion process of latex balloons is used as a comparative experiment. The experiment simulates grouting pressure using air pressure to determine the physical and mechanical properties of the soil samples before and after grouting. These properties serve as evaluation criteria for the effectiveness of building grouting uplift correction.

The experiment includes three control groups, measuring the initial state before grouting, the state after lifting by 4mm, and the state after lifting by 7mm. Physical and mechanical properties of the soil samples are determined, including moisture content, sample density, specific gravity, and shear strength.

#### 3.2 Experimental Apparatus

The experimental apparatus consists of three units: the load-bearing unit, the grouting unit, and the displacement monitoring unit.

(1) Load-Bearing Unit: The load-bearing unit consists of a steel container and weights. The steel container is composed of a piston, container cap, body, and a bottom perforated steel plate. The piston moves up and down for loading, while the perforated steel plate at the bottom facilitates drainage. The specific dimensions of the load-bearing unit are provided using a two-dimensional model established in AutoCAD, as shown in Figure 2. A three-dimensional assembly model with detailed drawings of various components is created using Solidworks for physical model fabrication, as depicted in Figure 3.

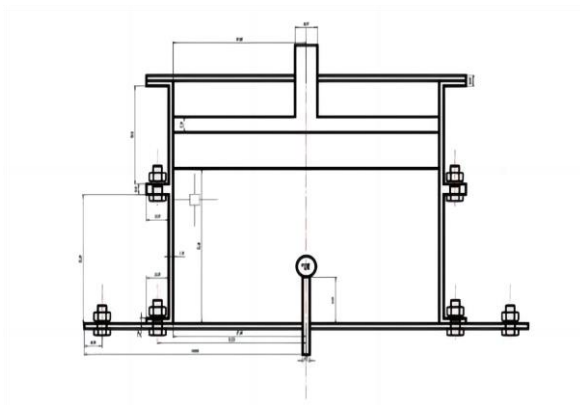
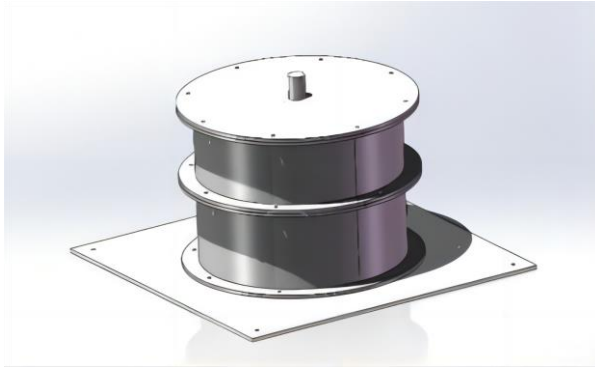


Fig. 2. AutoCAD 2D Device Schematic



**Fig. 3.** Solidworks 3D Assembly Model Schematic

(2) Grouting Unit: The grouting unit consists of four components: a latex balloon, a grouting pipe, a grouting hose, and a peristaltic pump. The grouting pipe has an outer diameter of 7.9mm, an inner diameter of 7.8mm, and a length of 75mm. It features a flanged top to enhance friction with the latex balloon and is equipped with steel hoops to ensure that the balloon remains securely in place, thus enhancing its integrity. The peristaltic pump is a reciprocating cyclic pump that increases air pressure to inflate the latex balloon, simulating the grouting effect.

(3) Displacement Monitoring Unit: The displacement monitoring unit comprises a graduated scale located inside the steel container body. This scale is used to determine the vertical displacement change of the soil by reading the values before and after the grouting experiment.

(4) Test Apparatus Assembly: The steel container was assembled and secured with bolts. The grouting pipe was installed and fixed 75mm above the bottom perforated plate. The upper end of the grouting pipe was connected to a thin-walled bladder, and the lower end was connected to the grouting hose. The other end of the hose was connected to a peristaltic pump, as shown in Figure 4.



**Fig. 4.** Experimental Equipment Physical Assembly Diagram

### 3.3 Simulated Grouting Experiment

In this experiment, the grouting process was designed to simulate ideal consolidation grouting, as illustrated in Figure 5. A thin-walled balloon was fixed at the upper part of the grouting pipe. Air was injected into the balloon through the grouting orifice to simulate the grouting process, with the peristaltic pump operating at 100 rpm.

The first crucial step is to finalize the air tightness test, then after the soil specimen preparation, the peristaltic pump switch was turned on. The pump initially evacuated air from the balloon until residual gases were removed. Then, the peristaltic pump's direction was reversed to inflate the balloon, initiating the simulated grouting process. The scale above the container was observed, and when the soil was raised to the target height, the switch was closed. Vertical displacement changes were recorded during the simulated grouting process.

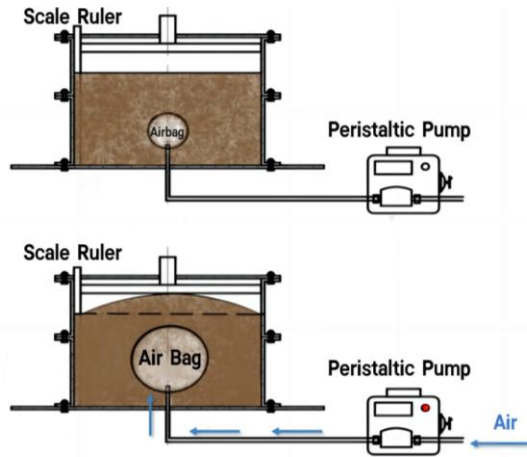


Fig. 5. Schematic Diagram of Simulated Grouting Test

### 3.4 Physical and Mechanical Property Tests

At different groups, including the initial state, 4mm uplift, and 7mm uplift, heterogeneous pivotal physical and mechanical property indicators of the soil sample were measured. Soil particle density was measured using the ring knife method, specific gravity was determined using the specific gravity bottle method, and moisture content was determined using the drying method.

Shear strength was determined through direct shear tests. Prior to shearing, the soil sample was subjected to consolidation to meet the stability standard requirements, with a consolidation time of 24 hours. After consolidation, the soil sample was sheared at a rate of 0.8mm/min under various vertical stresses (50kPa, 100kPa, 150kPa, 200kPa). After shearing, the critical state shear stress under the influence of each level of vertical stress was selected as the shear strength, and the critical state effective internal friction angle and cohesion were calculated based on the slope of the trendline.

## 4 Test results and discussion

### 4.1 Density and Moisture Content

**Table 1.** Density and Moisture Content Changes.

Uplift Displacement	Soil Density ( $\text{g}/\text{cm}^3$ )	Moisture Content (%)
0mm	2.146	20.04
4mm	2.246	19.47
7mm	2.276	19.40

From Table 1, it is palpable that the initial state of the soil sample had a higher density compared to the second group, which was raised by 4mm. The initial state had a density increase of  $0.1 \text{ g}/\text{cm}^3$  and a decrease in moisture content of  $0.57\%$ . Comparatively, the second group, raised by 4mm, had a density increase of  $0.03 \text{ g}/\text{cm}^3$  and a moisture content decrease of  $0.07\%$  when compared to the third group raised by 7mm.

As the grouting process continued, the density of the soil gradually augmented, and the moisture content gradually decreased. The changes in density and moisture content during the raising phase were relatively small. Furthermore, the changes in both density and moisture content after raising by 7mm were less significant than the changes observed after raising by 4mm.

### 4.2 Comprehensive Analysis of Specific Gravity, Density, Moisture Content, and Porosity

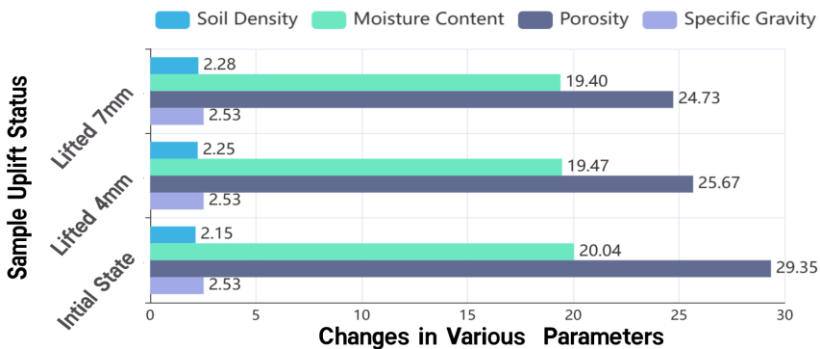


**Fig. 6.** Graph of Physical Property Indicators and Elevation Height Variation

According to the data analysis in Figure 6, it is evident that in the initial state, the soil surrounding the latex balloon was compacted, resulting in reinforcement around the soil sample. As lateral reinforcement reached saturation, the upper part of the soil began to rise. The grouting pressure was mainly used to lift the upper part of the soil, and its compaction effect on the surrounding soil was significantly reduced compared to the lifting effect. Therefore, the changes in soil density and moisture content were

less pronounced after raising by 7mm compared to the changes observed after a 4mm lift. This indicates that grouting and lifting have a certain reinforcing effect on the surrounding soil.

### 4.3 Shear Strength

Direct shear tests were conducted on soil samples in three states: initial, raised by 4mm, and raised by 7mm. The tests were performed under different loading conditions and the shear strength variations of the soil were obtained. Using the critical state shear stress under vertical stress as the shear strength, a relationship curve between shear strength and vertical pressure was fitted. This allowed the determination of the effective internal friction angle and cohesion at the critical stress, as shown in Table 2.

**Table 2.** Changes in Effective Internal Friction Angle and Cohesion.

Uplift Displacement	Internal Friction Angle (°)	Cohesive Strength (kPa)
0mm	8.28	12.07
4mm	17.26	16.31
7mm	19.56	17.66

Additionally, the fitted curves for shear strength versus vertical pressure (arranged from left to right in the order of initial, raised by 4mm, and raised by 7mm states) were integrated and compared.

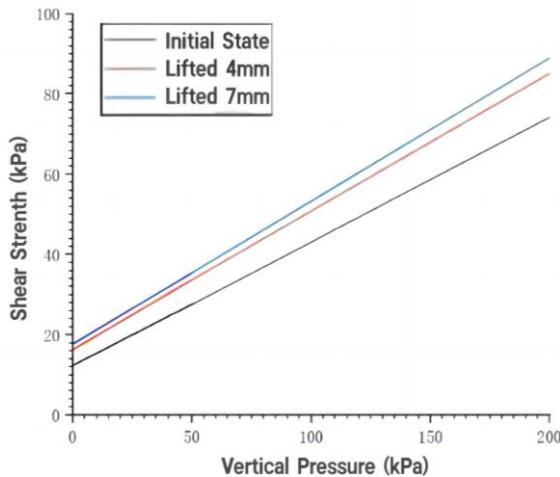


**Fig. 7.** Shear Strength vs. Vertical Pressure Relationship Graph

From Figure 7, it is evident that as the height of soil uplift increases, cohesion ( $c$ ) increases from 12.07 to 17.66, and the internal friction angle ( $\phi$ ) increases from 17.26 to 19.56. This increase in cohesion and internal friction angle enhances the soil's shear strength, affirming the reinforcing effect of the grouting and lifting method.

## 5 Conclusion

This study has analyzed the grouting and lifting mechanism, and through experimental simulations of real engineering grouting and lifting conditions, it has drawn the following conclusions based on changes in various physical and mechanical properties of soil samples under specific grouting pressures. A comprehensive analysis of these indicators has led to the following findings:

(1) The grouting and reinforcement process can be divided into two stages: the compaction of soil during the grout injection stage and the subsequent uplifting stage. These two stages together achieve both consolidation and the correction of the upper structure of the soil sample.

(2) During the 3mm-7mm uplift stage compared to the 0mm-3mm uplift stage, the increasing trends of various physical and mechanical properties of the soil sample weakened, indicating that there is a maximum reinforcement efficiency during the uplift process.

(3) In the initial state, the grouting pressure is primarily used to compact and reinforce the surrounding soil. As the grouting pressure increases, the soil sample begins to rise, and the grouting pressure is mainly used for uplifting the soil, which reduces the consolidation effect on the surrounding soil. The compaction effect diminishes significantly compared to the uplifting effect.

## References

1. Zhu H, Luo X, Peng F, Li X and Liu C 2017 Research on China's Urban Underground Space Planning and Development Strategy. *China Engineering Science* 19(06) pp 12-17.
2. Ge J. 2007 Research on the Analysis of the Causes of Tilting of Existing Buildings. *Shanxi Architecture* 28 pp 105-106.
3. Wu Z. 2022 Research on Correction and Reinforcement Techniques for Existing Buildings. *Sichuan Cement* 06 pp 149-151.
4. Li M, Zhang X, Li S, Zhang Q, Zuo J and Lan X. 2019 Calculation Method for Grouting and Lifting Based on Numerical Simulation and Model Experiments [J]. *Journal of Harbin Institute of Technology* 51(8) pp 159-166.
5. M Adel K E, M Tamotsu, H Keijiro, Hideo T and Hisashi F. 2022 Shallow Performance of Compaction Grouting. *Presentation Collection of Ground Engineering Research Presentation Meeting JGS37(0)* pp 1127-1128.
6. Wang G, Du M and Miao X. 2000 Research on the Mechanism and Effectiveness of Compaction Grouting. *Chinese Journal of Rock Mechanics and Engineering* 05 pp 670-673.
7. Nichols S C and Goodings D J. 2020 Physical Model Testing of Compaction Grouting in Cohesionless Soil[J]. *Journal of Geotechnical and Geoenvironmental Engineering* 126(9) pp 848-852



**Open Access** This chapter is licensed under the terms of the Creative Commons Attribution-NonCommercial 4.0 International License (<http://creativecommons.org/licenses/by-nc/4.0/>), which permits any noncommercial use, sharing, adaptation, distribution and reproduction in any medium or format, as long as you give appropriate credit to the original author(s) and the source, provide a link to the Creative Commons license and indicate if changes were made.

The images or other third party material in this chapter are included in the chapter's Creative Commons license, unless indicated otherwise in a credit line to the material. If material is not included in the chapter's Creative Commons license and your intended use is not permitted by statutory regulation or exceeds the permitted use, you will need to obtain permission directly from the copyright holder.

